NANO LETTERS

2007
Vol. 7, No. 9
2819−2823

One- and Two-Photon Excited Optical pH Probing for Cells Using Surface-Enhanced Raman and Hyper-Raman Nanosensors

Janina Kneipp,*,†,‡ Harald Kneipp,† Burghardt Wittig,§ and Katrin Kneipp†

Harvard University Medical School, Wellman Center for Photomedicine, Boston, Massachusetts 02114, Federal Institute for Materials Research and Testing, D-12489 Berlin, Germany, and Institute for Molecular Biology and Bioinformatics, Charite, D-14195 Berlin, Germany

Received June 13, 2007; Revised Manuscript Received August 2, 2007

ABSTRACT

We demonstrate spatially resolved probing and imaging of pH in live cells by mobile and biocompatible nanosensors using surface-enhanced Raman scattering (SERS) of 4-mercaptobenzoic acid (pMBA) on gold nanoaggregates. Moreover, we also show that this concept of pH nanosensors can be extended to two-photon excitation by using surface-enhanced hyper-Raman scattering (SEHRS). In addition to the advantages of two-photon excitation, the SEHRS sensor enables measurements over a wide pH range without the use of multiple probes.

In the vicinity of gold and silver nanoparticles, spectroscopic effects can be strongly affected due to coupling to surface plasmons[1] and enhanced local optical fields.[2] Raman scattering performed in local optical fields of silver and gold nanostructures, the effect of so-called surface-enhanced Raman scattering (SERS),[3,4] can result in effective Raman cross sections at the level of fluorescence cross sections of strong fluorophores.[5] Local optical fields also provide the key effect for the observation of surface-enhanced hyper-Raman scattering (SEHRS) at effective two-photon cross sections similar to or higher than the best cross sections for two-photon fluorescence.[6] Surface-enhanced Raman scattering measurements in cells are a topic of rapidly increasing interest, as they enable spatial resolutions that allow chemical probing of subcellular structures, collection times suitable for studying cellular processes, and the application of photostable probes and labels for multiplexing without dependence on a specific excitation wavelength.[7−9]

Gold and silver nanoparticles introduced into cells are nanosensors that can act in various complementary ways: (i) Gold nanoparticles or nanoaggregates can serve as biocompatible nanosensors that probe cellular chemistry in their local environment by delivering the enhanced Raman spectra of biological molecules and structures in their vicinity. In this way, information on the molecular composition of morphological units or structures in live cells can be obtained at high sensitivity and lateral resolution. By selectively enhancing the Raman signal from molecules in their immediate vicinity, gold nanoparticles have been used to directly probe the chemical composition of endosomes of different stages and for the detection of specific cellular molecules, such as adenosine monophosphate (AMP).[7] (ii) Gold or silver nanoparticles can serve in cells also as labels that highlight cellular structures based on the surface-enhanced Raman signature of a reporter molecule linked to them, e.g., a dye.[8,9] If the SERS spectrum of such a reporter molecule depends on the pH value in its environment, SERS nanosensors can act as pH probes.

SERS spectra of 4-mercaptobenzoic acid (pMBA) on silver and gold electrodes and the dependence of the spectra on the pH value have been reported and discussed in terms of adsorption geometry on the metal and on the state of dissociation of the carboxyl group as a consequence of surrounding pH.[10] Recently, the pH-dependent SERS spectra of pMBA adsorbed on gold nanoshells bound to a silicon substrate were used to create a pH meter working over the range of 5.8−7.6 pH units.[11] Similar experiments demonstrate that hollow gold nanospheres are responsive over a pH range of 3.5−9.[12] SERS studies on silver nanoparticle clusters functionalized with pMBA showed that the spectrum is sensitive to pH changes in the surrounding solution in the range of 6−8.[13] The authors conclude from a SERS spectrum

* Corresponding author. E-mail: jkneipp@janina-kneipp.de.
† Harvard University Medical School, Wellman Center for Photomedicine.
‡ Federal Institute for Materials Research and Testing.
§ Institute for Molecular Biology and Bioinformatics, Charite.

10.1021/nl071418z CCC: $37.00
Published on Web 08/16/2007

measured from these silver particles incorporated into Chinese hamster ovary cells that the pH in the environment of the particles was below 6, an observation consistent with the particles being located inside a lysosome.[13]

As will be shown in this work, SERS nanosensors can be used for sensitive pH imaging in individual live cells. Our nanosensor consists of gold nanoaggregates with pMBA attached, which enables biocompatible and mobile pH probing ideally suited for live cell studies. The SERS signal of pMBA can be analyzed in order to allow one to differentiate between various pH values within the endosomal compartment of a eukaryotic cell. Moreover, we will show here that the concept of a SERS-based pH sensor can be extended to two-photon excitation using surface-enhanced hyper-Raman scattering of pMBA. The pH sensor based on two-photon excitation benefits from excitation in the near-infrared, leading to reduced possible phototoxicity and stress to the cell, as well as the confinement of the two-photon interaction to the focus of the laser beam.[14,15] More importantly, SEHRS spectra of pMBA exhibit a spectral signature that allows an extension of the accessible pH range compared to a SERS sensor. In particular, a pH probe based on SEHRS signals has the potential to measure and to differentiate pH values in a more acidic environment, a pH range that is of particular relevance for studies of lysosomal and phagosomal compartments in cells.

Results and Discussion. Figure 1a illustrates the concept of the SERS nanosensor made from gold or silver nanoaggregates and an attached pH sensitive reporter. Information on the response of such a sensor to pH can be inferred from the signal ratio of different bands in the SERS spectrum at defined pH values. For pH imaging in live cells, pMBA was attached to gold nanoaggregates from aqueous pMBA solution at pH 6.5. To test the feasibility of these pMBA-functionalized metal nanoaggregates to act as pH sensors, they were suspended in aqueous solutions of different pH values. The pMBA spectra measured in these different pH environments are in agreement with previous reports and are discussed in more detail there.[10,13,11] Here, for illustration, Figure 1b displays SERS spectra of pMBA on gold nanoaggregates at pH values of 4.5 and 8.5. Strong lines at 1076 and 1586 cm^{-1} can be assigned to aromatic ring vibrations. The line at 1423 cm^{-1} belongs to the symmetric COO^- stretching mode and can be used as an indicator for the dissociation of the carboxyl group at higher pH values.[10] The shoulder at ~1700 cm^{-1} appears due to the C═O stretching vibration and intensifies at lower pH values. pMBA on silver nanoaggregates shows the same SERS spectra and the same pH dependence, except that the COO^- stretching mode is shifted to 1380 cm^{-1} (spectra not shown here).

The inset in Figure 1b displays the signal ratio of the 1423 cm^{-1} to the 1076 cm^{-1} band, obtained with gold nanoaggregates as a function of pH. As can be seen from this figure, the SERS signal of pMBA on gold nanoaggregates is sensitive to changes in the pH range between ~5.5 and 8. This is in agreement with the results reported for pMBA-covered immobilized gold nanoshells[11] and also with SERS data on pMBA on silver clusters.[13]

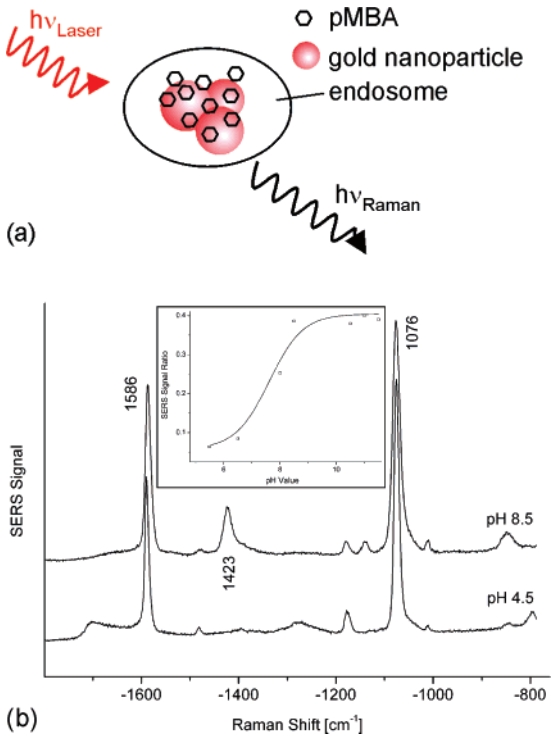

Figure 1. (a) Schematic of optical pH probing in live cells using a mobile and biocompatible pH sensor: Small nanoaggregates of gold colloidal particles covered with a reporter that provides a pH sensitive SERS signature are introduced into live cells and probe the pH in the surrounding endosome. (b) SERS spectra of pMBA on gold nanoaggregates at pH 4.5 and 8.5. The inset shows the ratio of the SERS signal at 1423 cm^{-1} relative to the signal at 1076 cm^{-1} as a function of pH. Spectra were collected in 100 ms using 785 nm cw laser excitation (10 mW). At pH values below 5.5, the signal of the COO^- stretching mode at 1423 cm^{-1} (1380 cm^{-1} for pMBA on silver) becomes too weak and cannot longer be used as a pH indicator. Above pH ~8, the ratio becomes constant, giving the upper end of the operating range of the pH SERS sensor.

To demonstrate the capability of a mobile pH sensor to probe and to image the pH values in single live cells, pMBA-covered gold nanoaggregates were added to the cell culture medium and introduced into the cell line NIH/3T3 by fluid-phase uptake. The experiments on cellular uptake are described in refs 7,16.

The photomicrograph in Figure 2 shows an example of a NIH/3T3 cell after 4.5 h incubation with the gold nanosensors. As can be seen in this picture, after an incubation of a few hours, numerous gold nanoparticles have accumulated in the cell. From ultrastructural studies of this and other cell lines, we know that, at this stage, many of the particles that were taken up by the cells through the process of endocytosis form accumulations in late endosomes and lysosomes.[7] They can be observed as black dots at the resolution of a light microscope. In our experiment, the cells were exposed to the pH nanosensors continuously for 4.5 h until the Raman experiments were carried out. Therefore, in addition, a portion of the pH nanosensors must also be located in early endosomes.

In the Raman microspectroscopic experiments with the cells, spectra were acquired by raster scanning over entire cells in steps of 2 μm. Excitation intensities $<10^5$ W/cm^2

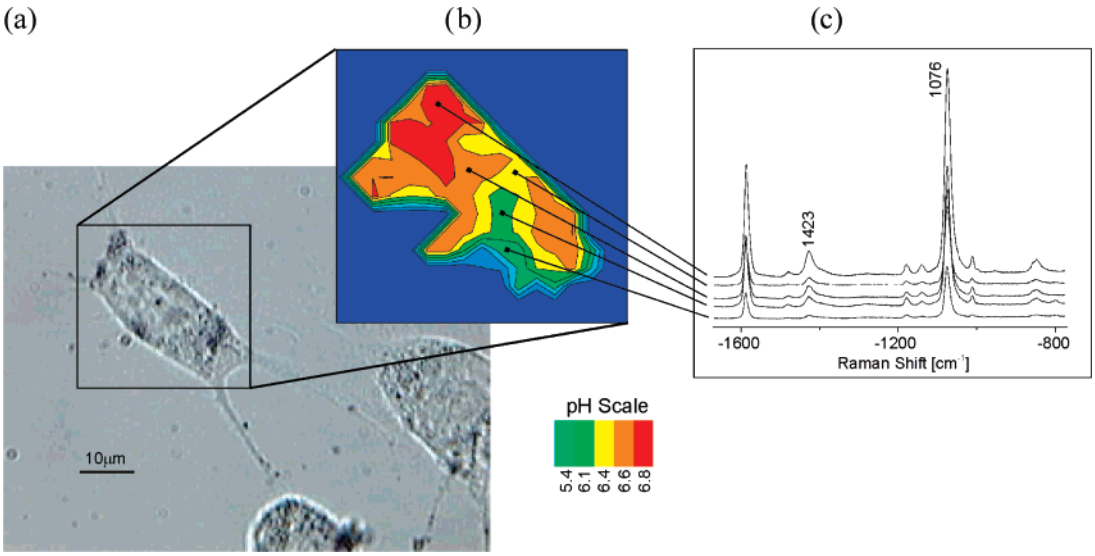

Figure 2. Probing and imaging pH values in individual live cells using a SERS nanosensor. (a) Photomicrograph of an NIH/3T3 cell after 4.5 h incubation with the pMBA gold nanosensor. Numerous gold nanoparticles have accumulated in the cell, enabling pH probing in different endosomes over the entire cell based on the SERS signature of pMBA. Lysosomal accumulations can be observed as black spots at the resolution of the light microscope. (b) pH map of the cell displayed as false color plot of the ratios of the SERS lines at 1423 and 1076 cm^{-1}. The values given in the color scale bar determine the upper end value of each respective color. Scattering signals below a defined signal threshold (i.e., where no SERS signals exist) appear in dark blue. (c) Typical SERS spectra collected in the endosomal compartments with different pH. The spectra were collected in 1 s each using 830 nm cw excitation (3 mW).

and collection times of 1 s per step ensured that the cells were viable during and after the measurement.[7,8] In accord with the assumption that nanosensor-containing endosomes are distributed all over the cytosol, a SERS signature of pMBA was measured in almost each of the spectra collected in the area of the cell. Other studies on pH nanosensors[11,13] as well as our experiments on nanoaggregates in solution have shown that a change in pH of the SERS nanosensors' environment causes an instant change of the spectral signature corresponding to the current pH value. The color map in Figure 2 displays the ratio of the SERS signals at 1423 and 1076 cm^{-1} as a function of sampling position in one of the cells, that is, a pH map of the cell. As illustrated by this example, the pH at different sampled spots in the cell, i.e., of the different endosomes that contained the pH sensors, varied between 6.8 and 5.4. It should be noted that the SERS sensor does not differentiate values below pH 5.4. Therefore, a lower pH can exist in the cellular areas assigned to 5.4. Typical unprocessed spectra collected in the areas with endosomes of the different pH values are displayed in Figure 2c. The variation of pH detected within the endosomal compartment of this and other individual cells is in agreement with the presence of nanosensor-carrying endosomes of different ages in this experiment. Assuming that the gold nanoparticle sensors follow the pathway of all internalized materials, which is known to be accompanied by an increasingly acidic pH in the endosomes of 3T3 cells,[17] we infer that the maximum observed pH of 6.8 is reported by sensors contained in early endosomes, whereas the lowest value of 5.4 and possibly below that we observe after 4.5 h represents the pH in late endosomes or lysosomes.

Determining intracellular pH with subcellular resolution is of particular importance for a better understanding of a broad range of physiological and metabolic processes. These include trafficking, recycling, and recruitment of intra- and extracellular molecules.[18−20] Intracellular pH varies between different compartments due to their specific functions but also over time within a compartment such as the endosomal. Defective endosome acidification plays a central role in a number of pathologies, among them cystic fibrosis,[21] pathologies of the kidney,[22] and certain cancers.[23] The regulation of endosomal pH can be important for the entry of viruses[24,25] and also in biotechnological applications such as nonviral gene delivery.[26,27] In many cell types, significant acidification compared to earlier endosomal stages takes place in the lysosome. There, to ensure, e.g., proper enzymatic function, pH can be well below 5, and even lower (<4).[28]

As shown in refs 11,13 (compare also Figure 1), the pH range below 5.4 cannot be further resolved because the SERS signatures are not sensitive to changes in this acidic range. However, this situation is changed for surface-enhanced hyper-Raman scattering (SEHRS).

Hyper-Raman scattering (HRS) is a two-photon excited Raman scattering process and thus results in Raman signals shifted relative to the doubled energy of the excitation laser.[29,30] The rather weak effect can be greatly strengthened if HRS takes place in the local optical fields of gold and silver nanostructures. As a nonlinear process, hyper-Raman scattering benefits to a great extent on enhanced local optical fields. SEHRS can exhibit effective two-photon cross sections on the order of $10^{-46}-10^{-45}$ cm^4 s. As a two-photon process, hyper-Raman scattering follows different selection rules resulting in a different spectral signature compared to Raman scattering. Figure 3a shows SEHRS spectra of pMBA on silver nanoaggregates obtained with 1.064 nm, picosecond excitation. For these experiments, pMBA-covered silver nanoaggregates were suspended into water of different pH

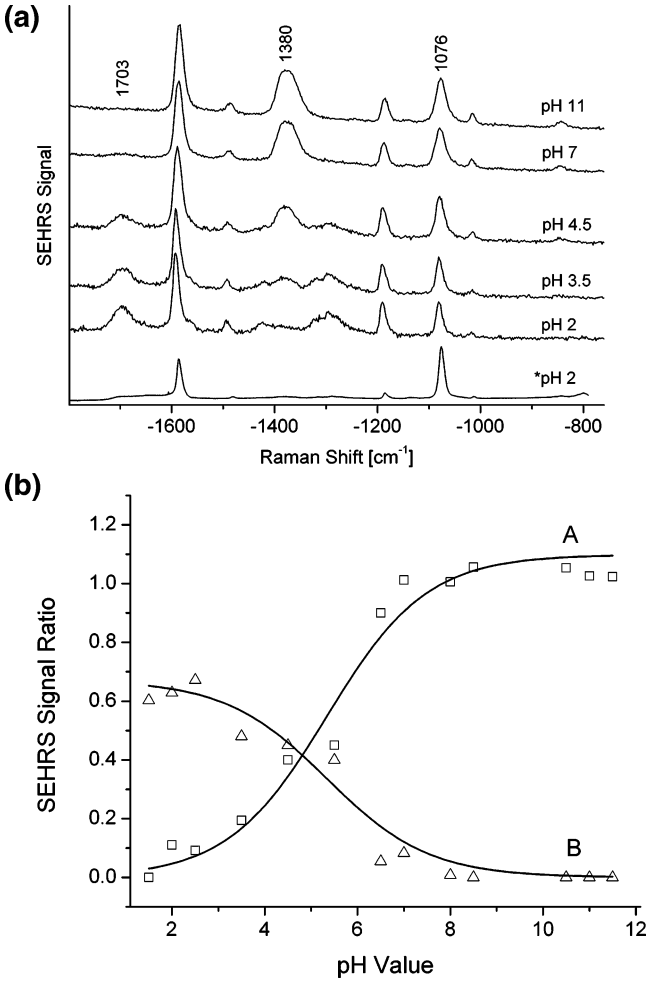

Figure 3. (a) SEHRS spectra of pMBA on silver nanoaggregates in different pH environment. Pronounced lines at 1380 and 1703 cm^{-1} allow one to infer information on pH over a wide operation range. For comparison, the bottom trace displays a SERS spectrum of pMBA on silver nanoaggregates at pH 2. SEHRS spectra were collected in 1 s using 1,064 nm ps excitation (peak intensities $\sim 10^{27}$ photons cm^{-2} s^{-1}). (b) Signal ratios at 1380 and 1076 cm^{-1} (A) and 1703 and 1076 cm^{-1} (B) plotted as a function of pH demonstrate the operation range of a SEHRS-based pH probe.

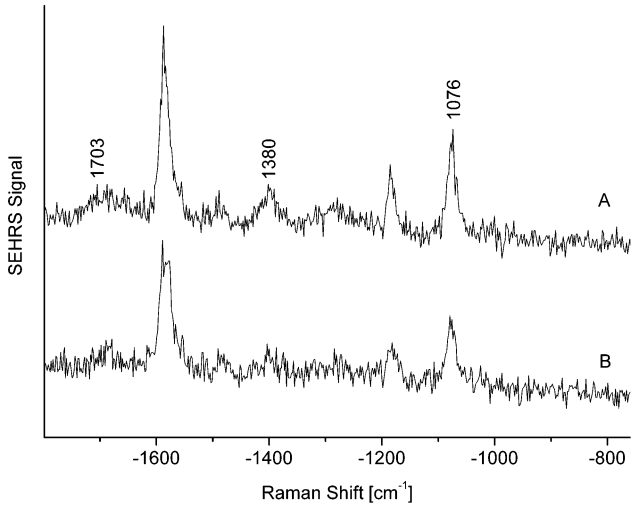

Figure 4. Typical SEHRS spectra of pMBA on silver nanoaggregates measured in an NIH/3T3 cell. Spectra were collected after a delay of >10 h delay after termination of the 4.5 h incubation with nanoparticles. Two-photon excitation was achieved with 1.064 nm mode-locked ps laser pulses (average power 10 mW, size of the laser spot ~ 2 μm, collection time 10 s). The spectral signatures indicate a variation between pH 4.9 and pH 4.5, consistent with the assumption that the time of the measurement most particles had accumulated inside lysosomes.

in the same way as for measuring the pH dependence of SERS. SEHRS spectra of pMBA show the same Raman lines as in SERS spectra, but the relative signal strengths of the bands are changed compared to SERS. These differences in the SEHRS signature of pMBA are very favorable for creating a pH sensor that allows measurements in a more extended range. Here we want to focus on two Raman lines: As the spectra in Figure 3 show, the line at 1380 cm^{-1} associated with the COO^- vibration appears at relatively high signal level compared to SERS (observed at 1423 cm^{-1}) and can therefore be followed down to lower pH values. Additionally, the 1700 cm^{-1} COOH stretching mode appears as pronounced strong band, which shows an opposite dependence on pH. Figure 3b displays the signal ratio of each of these two lines relative to the line at 1076 cm^{-1} as a function of pH value. On the basis of these two signals with opposite pH dependence, a SEHRS sensor can differentiate pH values over a wide range. This is of particular interest for measurements in subcellular compartments of extreme pH, e.g., very acidic lysosomes.

For a feasibility test of the SEHRS nanosensor in a more acidic biological environment, the pMBA-loaded silver nanoaggregates were introduced into the cell line NIH/3T3 by fluid-phase uptake as described for the SERS nanosensor. These preliminary experiments were done with silver nanoaggregates because of slightly better SEHRS signal strengths for this metal. In contrast to SERS imaging experiments in which cells were exposed to the pH nanosensors until the Raman experiments were carried out, SEHRS spectra were collected more than 10 h after finishing exposing the cells to the nanoparticles. At that time, almost all nanoparticles were supposed to have been accumulated in late endosomes or lysosomes.[7] In agreement with this, the SEHRS spectra collected in scans in these single cells show very similar spectral signatures. Typical spectra measured using mode-locked picosecond excitation at 1.064 nm are shown in Figure 4. A comparison of these spectra and others measured inside the cell with Figure 3 indicates pH values between 4.9 and 4.5. This is in very good agreement with pH values measured using fluorescence time-resolved techniques. In these experiments performed with the acidic lifetime probes DM-NERF dextrans, OG-514 carboxylic acid dextrans, and LysoSensor DND-160, the resting lysosomal pH value obtained from 3T3 fibroblasts was found to be between 4.5 and 4.9.[31]

Under our current experimental conditions, SEHRS spectra in cells were measured in 10 s collection time using an average power of $\sim$10 mW from a pulsed laser. These parameters are not yet suited for scans over live cells. Further optimization of SEHRS for pMBA on gold nanoaggregates can harness SEHRS pH nanosensors as a safe and biocompatible tool for application in live cells.

In conclusion, we have demonstrated pH imaging in single live cells at subendosomal resolution using SERS nanosensors. As expected, in NIH/3T3 cells, the SERS sensor indicates pH values between 6.8 for early endosomes and $\leq$5.4 and possibly below observed in late endosomes or lysosomes. Extension to two-photon excitation and exploiting pH sensitive SEHRS signals allows one to resolve and to differentiate pH values down to pH 2.

SERS/SEHRS pH nanosensors infer information using the relative signals of pairs of spectrally narrow Raman lines in the same spectrum. This allows quantitative measurements without any correction regarding cellular background absorption and emission signals. As was demonstrated here for pMBA, SERS and SEHRS provide strong signals also under electronically nonresonant excitation. This avoids photodecomposition of the sensor and allows free selection of the excitation wavelengths, optimized for the biological object under study. Other optical pH sensors based on one- or two-photon excited fluorescence signals, including also fluorescence lifetime measurements (see for example refs 32−34 and refs therein), in most cases require the application of multiple probes to cover wider pH ranges. In contrast to this, the same SERS/SEHRS sensor can operate between pH values of 8 and 2, and thereby enables probing of a variety of cellular compartments.

We have shown spatially resolved probing and imaging of pH in live cells by mobile and biocompatible nanosensors made from 4-mercaptobenzoic acid (pMBA) attached to gold nanoaggregates. The pH sensitive SERS of pMBA was analyzed in order to determine and to image the pH values in subcellular structures in the range from pH 6.8 to pH 5.4.

In a second step, we could successfully prove that the concept of a SERS pH sensor can be extended to two-photon excitation using surface-enhanced hyper-Raman scattering (SEHRS) of pMBA on nanoaggregates. Particularly for biological applications, the pH sensor based on two-photon excitation benefits from excitation at longer wavelengths in the near-infrared. Mostly important, SEHRS spectra of pMBA exhibit a spectral signature suited for measurements and differentiation of pH values between 8 and 2. The extended response range of the SEHRS pH sensor enables probing of a variety of subcellular compartments including those of extreme pH, e.g., very acidic lysosomes, without the use of multiple probes.

Acknowledgment. We are grateful to Irene Kochevar and Robert Redmond for providing us cell line NIH/3T3 and Chelvi Rajadurai for help with space in the cell culture facility. This work was supported by DOD grant no. AFOSR FA9550-04-1-0079 and by the generous gift of Dr. and Mrs. J. S. Chen to the optical diagnostics program of the Massachusetts General Hospital Wellman Center for Photomedicine.

Supporting Information Available: Preparation of pH nanosensors; delivery of the pH sensor into cells; pH imaging in cells. This material is available free of charge via the Internet at http://pubs.acs.org.

References

(1) Chance, R. R.; Prock, A.; Silbey, R. *J. Chem. Phys.* **1974**, *60*, 2744−48.
(2) Moskovits, M. *J. Chem. Phys.* **1978**, *69*, 1459−61.
(3) Jeanmaire, D. L.; VanDuyne, R. P. *J. Electroanal. Chem.* **1977**, *84*, 1.
(4) Albrecht, M. G.; Creighton, J. A. *J. Am. Chem. Soc.* **1977**, *99*, 5215−5217.
(5) Kneipp, K.; Wang, Y.; Kneipp, H.; Itzkan, I.; Dasari, R. R.; Feld, M. S. *Phys. Rev. Lett.* **1996**, *76*, 2444.
(6) Kneipp, J.; Kneipp, H.; Kneipp, K. *Proc. Natl. Acad. Sci. U.S.A.* **2006**, *103*, 17149−17153.
(7) Kneipp, J.; Kneipp, H.; McLaughlin, M.; Brown, D.; Kneipp, K. *Nano Lett.* **2006**, *6*, 2225−2231.
(8) Kneipp, J.; Kneipp, H.; Rice, W. L.; Kneipp, K. *Anal. Chem.* **2005**, *77*, 2381−2385.
(9) Wabuyele, M. B.; Yan, F.; Griffin, G. D.; Vo-Dinh, T. *Rev. Sci. Instrum.* **2005**, 76, 063710.
(10) Michota, A.; Bukowska, J. *J. Raman Spectrosc.* **2003**, *34*, 21−25.
(11) Bishnoi, S. W.; Rozell, C. J.; Levin, C. S.; Gheith, M. K.; Johnson, B. R.; Johnson, D. H.; Halas, N. J. *Nano Lett.* **2006**, *6*, 1687−1692.
(12) Schwartzberg, A. M.; Oshiro, T. Y.; Zhang, J. Z.; Huser, T.; Talley, C. E. *Anal. Chem.* **2006**, *78*, 4732−4736.
(13) Talley, C. E.; Jusinski, L.; Hollars, C. W.; Lane, S. M.; Huser, T. *Anal. Chem.* **2004**, *76*, 7064−7068.
(14) Zipfel, W. R.; Williams, R. M.; Webb, W. W. *Nat. Biotechnol.* **2003**, *21*, 1369−1377.
(15) So, P. T. C.; Dong, C. Y.; Masters, B. R.; Berland, K. M. *Annu. Rev. Biomed. Eng.* **2000**, *2*, 399−429.
(16) Kneipp, J. Nanosensors based on SERS for applications in living cells. In *Surface-Enhanced Raman Scattering: Physics and Applications*; Springer-Verlag Berlin: Berlin, 2006; Vol. 103, pp 335−349.
(17) Murphy, R. F.; Powers, S.; Cantor, C. R. *J. Cell Biol.* **1984**, *98*, 1757−1762.
(18) Maranda, B.; Brown, D.; Bourgoin, S.; Casanova, J. E.; Vinay, P.; Ausiello, D. A.; Marshansky, V. *J. Biol. Chem.* **2001**, *276*, 18540−18550.
(19) Zhang, A. S.; Sheftel, A. D.; Ponka, P. *Blood* **2005**, *105*, 368−375.
(20) Yates, R. M.; Hermetter, A.; Russell, D. G. *Traffic* **2005**, *6*, 413−420.
(21) Poschet, J. F.; Fazio, J. A.; Timmins, G. S.; Ornatowski, W.; Perkett, E.; Delgado, M.; Deretic, V. *EMBO Rep.* **2006**, *7*, 553−559.
(22) Hara-Chikuma, M.; Wang, Y. H.; Guggino, S. E.; Guggino, W. B.; Verkman, A. S. *Biochem. Biophys. Res. Commun.* **2005**, *329*, 941−946.
(23) Kokkonen, N.; Rivinoja, A.; Kauppila, A.; Suokas, M.; Kellokumpu, I.; Kellokumpu, S. *J. Biol. Chem.* **2004**, *279*, 39982−39988.
(24) Stuart, A. D.; Brown, T. D. K. *J. Virol.* **2006**, *80*, 7500−7509.
(25) O'Donnell, V.; LaRocco, M.; Duque, H.; Baxt, B. *J. Virol.* **2005**, *79*, 8506−8518.
(26) Walker, G. F.; Fella, C.; Pelisek, J.; Fahrmeir, J.; Boeckle, S.; Ogris, M.; Wagner, E. *Mol. Ther.* **2005**, *11*, 418−425.
(27) Chowdhury, E. H.; Maruyama, A.; Kano, A.; Nagaoka, M.; Kotaka, M.; Hirose, S.; Kunou, M.; Akaike, T. *Gene* **2006**, *376*, 87−94.
(28) Montcourrier, P.; Mangeat, P. H.; Valembois, C.; Salazar, G.; Sahuquet, A.; Duperray, C.; Rochefort, H. *J. Cell Sci.* **1994**, *107*, 2381−2391.
(29) Denisov, V. N.; Mavrin, B. N.; Podobedov, V. B. *Phys. Rep.* **1987**, *151*, 1.
(30) Ziegler, L. D. *J. Raman Spectrosc.* **1990**, *21*, 769−79.
(31) Lin, H. J.; Herman, P.; Lakowicz, J. R. *Cytometry Part A* **2003**, *52*, 77−89.
(32) Lin, H. J.; Herman, P.; Kang, J. S.; Lakowicz, J. R. *Anal. Biochem.* **2001**, *294*, 118−125.
(33) Hanson, K. M.; Behne, M. J.; Barry, N. P.; Mauro, T. M.; Gratton, E.; Clegg, R. M. *Biophys. J.* **2002**, *83*, 1682−1690.
(34) Bizzarri, R.; Arcangeli, C.; Arosio, D.; Ricci, F.; Faraci, P.; Cardarelli, F.; Beltram, F. *Biophys. J* **2006**, *90*, 3300−3314.

NL071418Z